Proceedings of ASME Turbo Expo 2016: Turbomachinery Technical Conference and Exposition
GT2016
June 13 – 17, 2016, Seoul, South Korea

GT2016-56308

ROTATING HEAT TRANSFER MEASUREMENTS ON A MULTI-PASS INTERNAL COOLING CHANNEL – I RIG DEVELOPMENT

Fabio Pagnacco, Luca Furlani, Alessandro Armellini, Luca Casarsa
Università degli Studi di Udine
Dipartimento di Ingegneria Elettrica Gestionale e Meccanica
33100 Udine, Italy
Email: luca.casarsa@uniud.it

Anthony Davis
Siemens Industrial Turbomachinery Ltd
Ruston House, Waterside South, LN5 7FD
Lincoln, England

ABSTRACT

The present contribution describes the design and realization of a rotating test rig for heat transfer measurements on internal cooling passages of gas turbine blades. The aim is to study the effects of Coriolis and buoyancy forces on the heat transfer distribution inside realistic cooling schemes.
Spatially resolved heat transfer data are obtained by means of transient thermochromic liquid crystals (TLC) technique. In order to replicate the same buoyancy effects induced by the Coriolis forces during rotation, the transient measurements are performed with a cold temperature step on the coolant flow. New solutions are adopted to generate the cold temperature step, acquire the experimental data on board of the rotating test model and to control the experimental parameters during tests execution. The main components of the rig will be described in the paper, together with an overview of the data processing methodology that has been developed.

INTRODUCTION

Safe and efficient operation of gas turbine engines strongly relies on effective blade cooling. Consequently, the performance required to the cooling systems is ever increasing, which leads to the definition of passage geometries that are increasingly complex. The design of such complicated devices by exploiting CFD tools is still a challenging task and therefore reliable experimental data are necessary for validation and verification purposes. These needs can only be satisfied if experiments replicate the real working conditions, with particular attention dedicated to the correct reproduction of the rotational effects and the ability to accommodate large test sections that reproduce full blade cooling schemes. Consequently, the demand on size and capabilities of dedicated test rigs is highly increased. The task is to develop facilities where detailed thermal analysis can be performed under rotation at engine similar conditions.

CURRENT STATE-OF-ART

Heat transfer measurement is based on the determination of the local surface temperature, which can be accomplished in several ways. Probably the simplest way to do it is to make use of thermocouples installed on the measurement surface. Examples of the application of this method can be found in the contributions by [1-2]. The main drawback of this method is the spatial resolution achieved, which is usually not sufficient to investigate local heat transfer distributions generated by passage features (i.e. ribs, pins).
Infrared cameras can be used for heat transfer measurement [3]. However, the difficulties in manufacturing test models with walls transparent to infrared radiation can limit substantially the application of this method for very large or complex geometries.
One of the most widely used methods for heat transfer measurements is liquid crystal thermography (LCT). With respect to other methods, LCT technique is characterized by having high spatial resolution, it can be performed on very complex surfaces, and finally it provides accurate measurements without requiring expensive devices. Two different methodologies can be followed, i.e. steady or transient LCT. An example of steady LCT applied to blade cooling passages can be found in Mayo et al. [4], which describe the analysis of convective heat transfer distribution in a rib-

roughened internal cooling channel at different rotation and Reynolds numbers.
The main disadvantage of steady measurements is the difficulty in providing an accurate estimate of the heat transfer losses through the test model surface, which becomes more significant for rotating experiments.
The transient method is more complex compared to the steady state method, but it overcomes the problem of heat losses characterization, moreover it requires much shorter testing time and hence is more suitable to carry out measurements under rotation. Waidmann et al. [5] investigated on heat transfer distribution in a two-pass internal cooling rib-roughened channel with engine-similar cross-section. For this study, the transient TLC technique was used only for stationary measurements.
Other contributions using the transient TLC technique used for stationary measurements are [6-7].
The key point of transient tests is to impose a temperature step to the coolant flow in order to activate the heat transfer process, and hence provide the boundary conditions used to compute the heat transfer coefficient distribution on the investigated surfaces [8]. The main issue about the use of this technique for rotating tests is that a cold temperature step on the cooling flow is required in order to match the same buoyancy effects found in real working conditions. Unfortunately, this increases the technical complexity of the system, indeed to provide a hot step is rather simpler and can be obtained by widely used mesh heaters. In the present contribution, a new solution to generate the cold temperature step has been developed and is described in detail.
Additional technical issues that had to be solved are related to the onboard viewing system that is required to record the liquid crystal phase change, the synchronization of this system with the flow temperature acquisition, the data management and communication with the stationary control system. Particular care was also put in the control of the experimental parameters (namely Reynolds and rotation numbers), which resulted in a feedback control system to drive the whole facility.
The aim of the paper is to describe in details the characteristic of the rig design and of the adopted technical solutions.

NOMENCLATURE

Bo	buoyancy parameter
c	
d_h	hydraulic diameter
h	heat transfer coefficient
$\dot{m}$	coolant mass flow rate
Nu	Nusselt number
R	rotation radius
Re	Reynolds number
Ro	rotation parameter
T_b	bulk temperature
T_{he}	temperature at the outlet of heat exchangers
T_w	wall temperature
TDA	control points of the TLC time peak search
TDB	
TDC	
TTL	0-5V signal (Transistor-Transistor Logic)
U_b	bulk flow velocity
μ	air dynamic viscosity
ρ	air density
Ω	rotational speed

RIG CHARACTERISTICS

GENERAL OVERVIEW OF THE TEST RIG

A view of the rig can be seen in Fig. 1 and a simplified sketch is provided in Fig. 2. A steel load bearing structure is used to support the transmission to the rotating arm, which spins around a vertical axis. A 5 kW electric motor is fastened to this structure and drives, through a transmission belt, a rotating joint bolted to the rotating arm. The rotating joint comprises a hollow steel shaft, which allows the airflow through the inner part, and is equipped with 32 slip rings on the outer side in order to provide electrical supply and signal connections to the rotating equipment.
The rotating arm is made of aluminum profiles. The test section is fastened on one side of the rotating arm by means of two aluminum supports, while on the opposite side counterweights are installed in order to balance the whole structure during rotation.
In the final setup of Fig. 1 the dimensions of the rotating arm are: 1500x600x700 mm, where a volume of 890x440x610 mm dimensions is made available to install the test section. The maximum allowable weight of the rotor (comprising test model, on board instrumentation, counterweights, etc.) is 2000N and it can be spun up to 400 rpm.

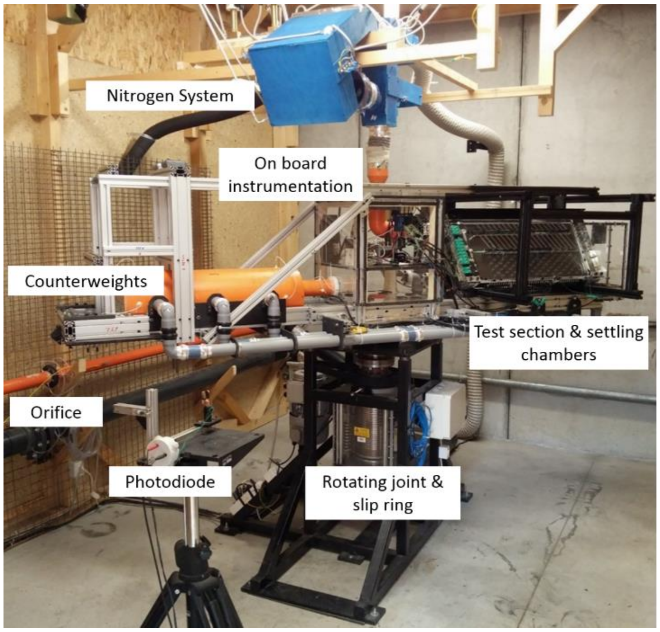

Figure 1: Test rig

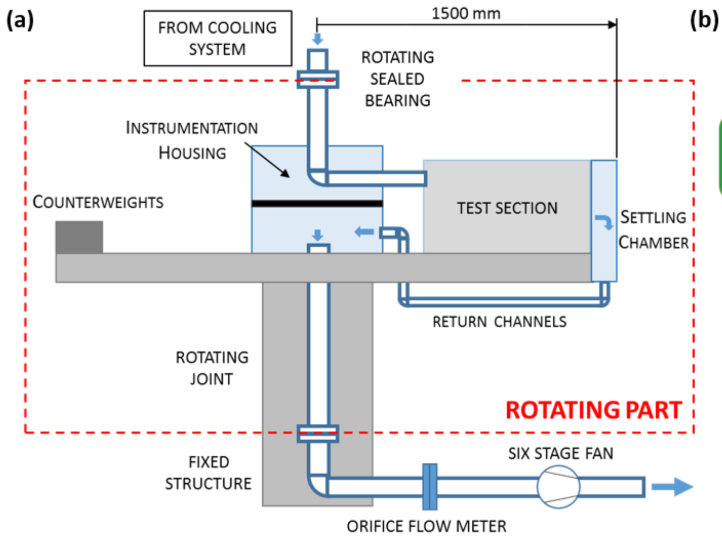

Figure 2: Test rig sketch (a), cooling system detail (b)

The cooling flow rate is obtained by sucking air using a six stage centrifugal fan connected to the hollow shaft of the rotating joint. The measurement of the airflow rate is obtained by an orifice flow meter located upstream of the fan.
The vision system that is used to acquire the images of the liquid crystals is installed on board of the rotating arm. This choice avoids the problems that can arise with the use of a stationary system, i.e. the synchronization of the image acquisition with the system rotation and the loss of image quality due to blurring effects caused by rotation. However, on board systems may pose some limitations to hardware dimensions, weight and difficulties associated with the data storage and system control. For details about the adopted video system the reader should refer to the section dedicated to its description.
Finally, pressure and temperature values of the flow field inside the rotating equipment can also be measured by means of dedicated devices installed on the rotor. A Wi-Fi bridge provides the communication with the ground control unit.
The key point of transient tests is to impose a temperature step to the coolant flow in order to activate the heat transfer process, and hence provide the boundary conditions used to compute the heat transfer coefficient distribution on the investigated surfaces. The main issue about the use of this technique for rotating tests is that a cold temperature step on the cooling flow is required in order to match the same buoyancy effects found in the real applications.
These requirements have been satisfied by the design of an ad-hoc cooling system that makes use of liquid nitrogen. The latter is essentially composed of fin and tube heat exchangers and a dedicated switching valves unit. More details will be provided in the next section.
Due to the very large variation of flow temperature that occurs during the test phase, physical properties of the cooled fluid change, which causes a variation of both Re and Ro parameters. In order to maintain constant Reynolds and Rotation parameters, a feedback control system has been developed. This system has the task to control simultaneously the air-cooling flow rate and the rotational speed of the test section.

NITROGEN SYSTEM

The main reasons that pushed for the use of a N_2 based cooling system instead of more conventional chiller units are the wider range of working conditions easily achievable and the overall reduced cost. The natural drawback of this choice is that a dedicated design has been required for both system components and control devices.
Figure 2(b) provides a sketch of the main components of the cooling system, namely N_2 storage, heat exchangers, and control valves unit. The cooling system is connected to a pneumatic rotating joint in order to deliver the flow to the test section. The connecting uncooled pipe length is approximately 800mm.
The heat exchanger unit is composed by a rectangular channel in which three fin and tube heat exchangers are installed in sequence and are supplied with liquid nitrogen from a 500 liter reservoir. Liquid nitrogen flow is controlled by a remotely driven gate valve and it is regulated by a needle valve. Additional automatic valves are installed in the nitrogen pipes for safety reasons in the occurrence of cryogenic trap.
Ambient air flows through the first heat exchanger, which has a tighter fin pitch and a wider cross sectional area with respect to the other two heat exchangers. Air starts to cool down to about 5°C and hence the great part of the air humidity content can condensate. The nitrogen is initially fed to the 3rd heat exchanger in the unit, then the 2nd, hence, being the coldest, they have the task to chill the air down to the minimum allowable temperature (about -80°C) and to extract the remaining water content from air that freezes on the heat exchanger fins. A wide fin pitch helps preventing from blockage caused by frost.

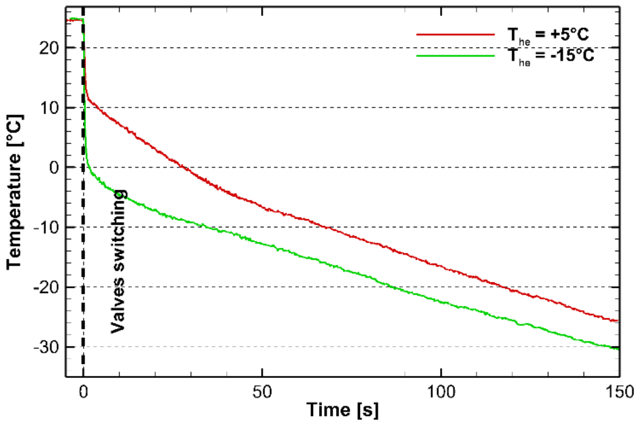

Figure 3: Achievable temperature steps at the inlet of the test section

The switching valves unit, shown in Fig. 2(b), is located in between test and heat exchanger sections, and it is necessary in order to impose the temperature step to the cooling air. The unit comprises three pneumatic valves remotely controlled, which enables two working conditions: pre-cooling and test phases.
In the pre-cooling phase, both auxiliary valves are open while the principal one is closed. In this way, test rig and nitrogen system are decoupled. Ambient air flows through the auxiliary inlet into the test section in order to reach initial isothermal steady conditions. Meanwhile, an auxiliary fan sucks ambient air through the heat exchangers in order to cool down the system and reach target conditions for the experiments.
The simultaneous switching of the three valves (auxiliary valves close, principal valve opens) sets the test phase starting point and air chilled by the heat exchanger flows through the test section producing the temperature step. When the auxiliary valves are closed, a dilution hole in the auxiliary line prevents from vacuum condition in the valve system that can be source of leakage or structural failure.
Figure 3 shows examples of the achievable temperature profile at the position in the rotor where the test section inlet will be located. Two profiles have been obtained with different settings of the cooling system, which in turn results in different temperatures at the exit of the heat exchangers (T_{he}). The values of T_{he}=+5 and -15°C referenced in the figure are the temperature of the flow at the exit of the cooling system and at the beginning of the test /end of the pre-cooling phase and they will continue to lower during the test phase. They have been used to successfully test a multi pass channel with liquid crystals with activation temperatures of 12°C and 2°C [11].

ACQUISITION SYSTEM

<u>On board</u>

Images acquisition

Two digital cameras, a fan-less pc, and four halogen lamps compose the image acquisition system. The key features that the cameras must satisfy for the specific application and that drove the device selection procedure are listed in the following.

- Cameras have to be mounted on board the rig rotor, hence their size has to be minimal, in order to reduce weight and encumbrance.
- A strict constant frame rate is required. This requirement can be met only with externally triggered cameras.
- Reconstruction of the color signal history of each pixel of the image for the whole duration of the experiment requires constant camera settings (particularly exposure time and channel gains), so the choice must focus on cameras with customizable settings.
- Optics properties have to be taken into account as well. The restricted distance between the test section and the cameras leads to the use of wide angle lenses. Commercial compact cameras are mainly provided by non-customizable optics characterized by fisheye lenses, hence the need for custom optics that ensure a reduced image distortion with respect to fisheye lenses and customizable iris and focus settings.
- Halogen lamps have to be placed in order to guarantee an adequate illumination of the measurement area, however their positioning has to be made taking into consideration the minimization of the radiation effect (i.e. the lamps are quite far away from the surface and inclined). An aluminum struts frame integral with the rotating arms allows light positioning for different test section geometries and according to the above requirements (see [11] for more details).

Data storage is another consideration in the selection of the vision system. In the present design, the cameras are connected to a fan-less pc mounted on board the rotor that has the function to store the acquired images and to control the cameras.
With these requirements in mind, two Basler acA1300-60gc cameras were selected for use, with dedicated camera control software developed in LabView.

Temperature acquisition

Bulk flow temperature variation inside the test section is measured using K type thermocouples, with a diameter of 0.075mm in order to guarantee a quick response to temperature variations and a good accuracy in the temperature range of -90°C/+30°C. Thermocouples of thinner junctions (0.05mm) were also considered, but limited availability and higher cost, together with a no significant improvement of the response time excluded this option.
Thermocouples signals are acquired by a National Instruments cRIO with two NI 9213 thermocouple modules. Each of these modules allow up to 16 thermocouples to be acquired with a sampling rate up to 75 Hz, which is sufficiently high to ensure a good temporal discretization of the temperature variation.

Pressure acquisition

A 16 channel pressure scanner (NetScanner System mod.9116) is used to monitor and acquire pressure signals inside the test model and in specific locations of the air circuit.
The pressure scanner range is 25mbar with respect to a reference pressure, which can reach a maximum value equal to 100mbar. The data acquisition is synchronous with temperature

acquisition thanks to a TTL signal generated by the National Instrument cRIO.
The pressure scanner is mounted as part of the rotating equipment, as close as possible to the rotation axis, which is aligned with the transducers axis. In this way, the pressure scanner readings are not affected by the centrifugal forces due to rotation.

Static equipment

The stationary equipment is principally composed of the instrumentation necessary to supply and control the test rig.
A six stage centrifugal fan is used to provide the correct airflow rate to the test section. The electric motor (5kW) of the fan is driven by a remotely controlled inverter. Airflow to the cooling system heat exchangers is provided in the pre-cooling phase by a single stage centrifugal fan, the rotational speed of which is manually set. A remotely controlled inverter is also used to drive the electric motor that drives the rotor.
The coolant flow rate is measured by a calibrated orifice flow meter (UNI EN ISO 5167-2 standard). Orifice pressure and temperature signals (needed to compute the mass flow rate) are acquired by a National Instruments cDAQ, which is also used for the feedback control of the experimental parameters (see next section). Finally, the rotor angular velocity is monitored by sampling the TTL signal from a photodiode periodically screened by a target mounted on the test section. The signal is sampled by a counter board operated at a frequency of 20 MHz. The time lapse occurred between two successive rising edges of the photodiode signal is used to get in real time the mean angular velocity for each revolution.
The rig functionality is committed to three PCs with the following specific functions:

- on board pressure and temperature measurements and display (necessary to determine when steady thermal conditions are reached inside the channel during the pre-cooling phase);
- communication with the camera fanless PC, trigger the experiment start;
- monitor and control the experimental parameters (Re and Ro).

CONTROL SYSTEM

The control system has two functions:

- to trigger and to synchronize the on board acquisitions (TLC images, flow temperature and pressure signals);
- to control the experimental parameters during the test phase.

The first target uses National Instruments myDAQ clocking module, the generated trigger signal is used by the cameras and the cRIO, which in turns generates a TTL signal for the pressure scanner acquisitions, hence images, temperature, and pressure signal starts simultaneously and with the same temporal base.
As previously mentioned, control of flow rate and rotational speed is used to keep constant Re and Ro throughout the test period. This is accomplished by a control loop implemented on the NI cDAQ platform that receives input signals about:

- peripheral velocity (obtained by sampling the photodiode signal, see above);
- pressure and temperature signals from the orifice flow meter, the data are used by the control software to compute the actual flow rate;
- temperature and pressure values inside the test section measured at the location where the definition of Re and Ro values is made (e.g. inlet of the test section). These values are used to compute the coolant physical properties (i.e. density and viscosity). Signals are delivered to the ground control unit via the slip rings.

The output signals are the control voltage to the inverters that

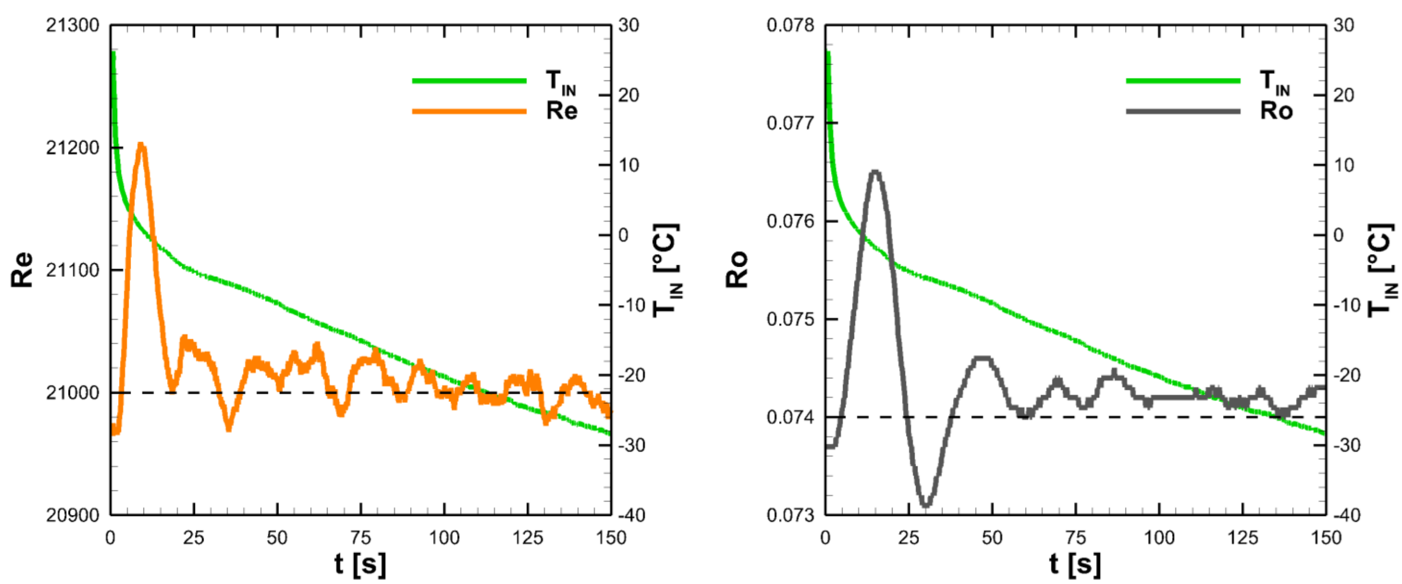

Figure 4: Example of test parameters control during the experiment, T_{IN} is the flow bulk temperature at the channel inlet.

drive the rig rotor and the six stage centrifugal fan. A PID controller is used to control the flow rate, because of the quick dynamic response of both the six stage fan and of the measurement systems involved in the control (pressure and temperature at the orifice). Conversely, a proportional controller is sufficient to regulate the rotational speed in view of the high inertia of the rotor and also because the rotor velocity has to decrease monotonically during the test. An example of how the control system works is reported in Fig. 4. It can be seen that the control systems acts on the test parameters throughout the test keeping them constant, within a 0.7% margin of error for the Ro and 0.2% for the Re, after an initial overshooting, due to the abrupt change in flow temperature (see as an example the variation of the channel inlet temperature T_{IN} in Fig. 4).

ACHIEVABLE TEST CONDITIONS

The heat transfer process in rotating cooling channel is dominated by the following non dimensional parameters:

$$Nu = f(Re, Ro, Bo, Pr, Ma) \tag{1}$$

Heat transfer distribution from tests on scaled model can be projected on real application only if similarity of these parameters is ensured between rig and engine.
The dependency on both Prandtl and Mach numbers can be neglected, since rig and real applications are working with air in subsonic regimes. The remaining parameters, i.e.: Reynolds, rotation and buoyancy numbers, cannot be set independently to each other, due to their definitions:

$$Re = \frac{\rho U_b d_h}{\mu} = \frac{\dot{m}}{d_h \mu} \tag{2}$$

$$Ro = \frac{\Omega d_h}{U_b} = \frac{\Omega \rho d_h^3}{\dot{m}} \tag{3}$$

$$Bo = \frac{\Delta\rho}{\rho} Ro^2 \frac{R}{d_h} = \frac{T_w - T_b}{T_b} Ro^2 \frac{R}{d_h} \tag{4}$$

$$d_h = \frac{4 \text{ cross section area}}{\text{cross section perimeter}} \tag{5}$$

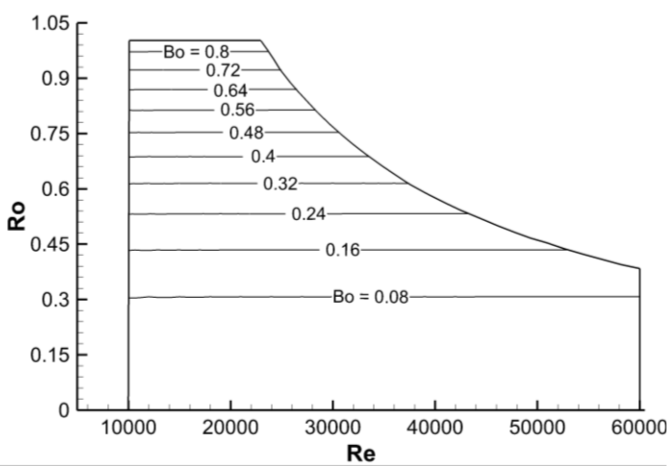

Figure 5: Achievable test conditions

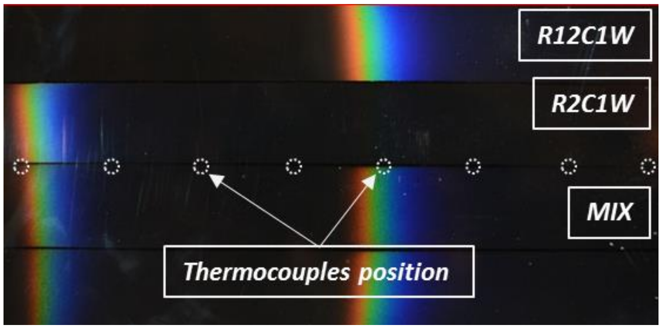

Figure 7: Liquid crystals calibration image.

Consequently, in the rig application, once the technical limitations of the rig have been defined (max rpm, temperature range, available flow rate), a map of possible test conditions is uniquely defined.
As an example, the map in Fig. 5, refers to a model of square section of d_h=75mm, placed at 850mm from the axis of rotation.

EXPERIMENTAL PROCEDURE

DATA PROCESSING

CALIBRATION

Liquid crystal calibration

A typical ex-situ calibration slab is used to perform the calibration of liquid crystals. More complex in-situ calibration is not required since narrow banded liquid crystals will be used and, therefore, accuracy issues related to viewing angle and illumination are negligible.
The main issue of the calibration is to ensure the low activation temperature of the liquid crystal, which can be very close to 0°C. To accomplish this, on one side of an aluminum slab a cold sink is generated by using two 100W Peltier cells, connected in series (Fig. 6). To make them work close to the maximum efficiency, the hot side is cooled by means of a finned plate water heat exchanger. The hot sink on the other side of the aluminum slab is obtained with a similar set-up as the cold sink. By acting on the DC supply voltage to the various Peltier cells, different gradients can be re-created inside the metallic slab with a temperature range of -15°C/+20°C.

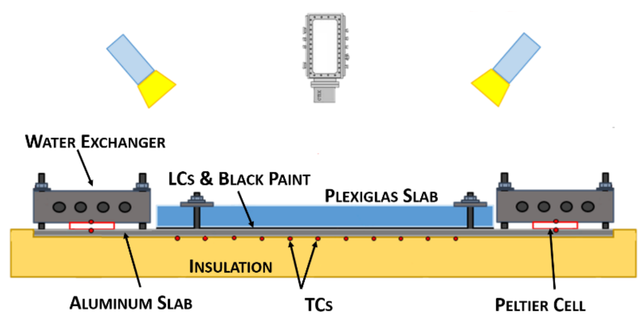

Figure 6: Liquid crystals calibration plate

The liquid crystals to be calibrated are sprayed on a Plexiglas slab and then covered with black paint to increase the contrast. The Plexiglas slab is pressed tightly on the aluminum slab in order to place in contact the two surfaces and to avoid insulating air bubbles.
Under the plate, twelve thermocouples are installed in known locations, inside holes drilled close to aluminum surface. These thermocouples are used to acquire the temperature of the aluminum surface that is assumed to be representative of the liquid crystals temperature.
To acquire the image of the calibration area, a camera and a lighting setup similar to the test rig setup is used.
The test sections that are about to be investigated are complex and are characterized by a strong variation of the heat transfer coefficient. Therefore, a mixture of two liquid crystals with different activation temperatures will be used. The calibration procedure is also useful to verify possible effects on the phase change process of the liquid crystal due to the mixing. In Fig. 7, a typical calibration image is reported. This example refers to two narrow banded encapsulated liquid crystals supplied by Hallcrest and with activation temperature of 12°C (R12C1W) and 2°C (R2C1W), respectively. It is possible to observe how the mixing process does not alter the liquid crystals optical properties.

Camera calibration

The tradeoff between camera field of view, lens distortion, and camera distance resulted in the choice of using 2 cameras to frame the surface corresponding to the maximum test section dimension, i.e. 400x800 mm (an example of a raw image acquired by one camera is shown in Fig. 8). The drawback is the need of a reliable procedure of image de-warping and measurement area reconstruction. Moreover, the computation of the T_b distribution has to be performed on the complete domain (see next section), therefore it is necessary to be able to correctly merge the images of the two cameras to get an accurate reconstruction of the domain. The procedure is furtherly complicated by computing memory constraints that prevent the processing of the whole images in a single step. Consequently, the image of each camera is split in multiple sub-areas (usually 3) that are re-combined together at the end of the computation.
The requirements needed for this procedure are:

- de-warp highly deformed images obtained by using wide angle lenses;
- reconstruct the measurement area obtained with multiple cameras;
- associate the images to the "CAD space" in order to correlate pixel-to-real positions.

A two-step de-warping procedure has been implemented. The first step is used to account for lens distortion. An image of a dotted grid placed on the model external surface is acquired and by means of commercial software the dots position in image coordinates (px) is recognized and associated to the real position on the grid. An in-house developed de-warping software, computes de-warping polynomials coefficients that

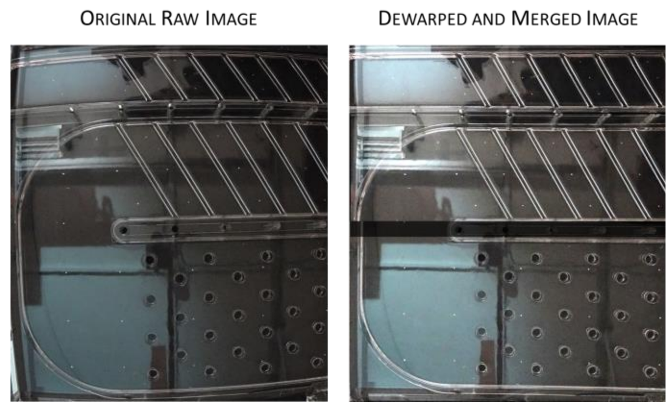

Figure 8: examples of raw distorted image (left) and dewarped and reconstructed image (right).

are used to obtain a first roughly de-warped image. The second step of this procedure is a refinement that takes into account for the distortion associated to the thick Plexiglas wall of the test section. The procedure and methodology is basically the same as for the first step but with the difference that dots drawn at known positions on the inner surface of the test section are used as control points. These points are used also as reference points to merge the de-warped images from the two cameras. An example of the final result is given in Fig. 8.

PROCESSING SOFTWARE

Starting from the acquired images sequences and thermocouples readings, the processing software operates on two different macro objectives: the determination of the liquid crystals activation time and the T_b computation on the measurement domain.
The activation time determination is based on the search of the maximum of the green signal intensity for each pixel of the acquired images. In order to reduce the number of pixels that has to be computed, and hence the computational time, a user mask definition tool has been developed. In this way, the user can select only the areas that are useful for the Heat Transfer Coefficient (HTC) evaluation, excluding "a priori" areas of no interest (e.g. rib surfaces, lateral walls, etc.).
After that, an automatic multi band peak finding procedure can be performed. The requirements on which the peaks searching algorithm has been developed are:

- identification of peaks from multiple liquid crystals;
- accurate identification of peaks of very different morphology (amplitude and shape);
- fully automatic peak search with the minimum requirement of user defined parameters, in order to make the procedure fast and effective independently by the nature and quality of the raw signal.

The procedure involves a sequence of operations. Firstly, the signal is analyzed in order to search for the number of active peaks. A recursive procedure based on the analysis of the first derivative of the signal has the target to define the number of

peaks, which represent the number of active liquid crystals, and their raw position in time. For each peak, three characteristic points of the signal are defined (see Fig. 9): first derivative maximum (TDA), first derivative zero (TDB), and the zero of the linearization around TDA (TDC). The distance between points TDA and TDC, can be seen has a rough estimation of half of the peak time duration (activation interval). At this point, a first validation step is performed in order to eliminate bad signals. A signal is rejected if it does not meet two criteria: the peak amplitude must be higher than a prescribed threshold and the signal first derivative must be negative after the peak location and within the activation interval above identified. Once the peaks have been roughly identified with the procedure of above, the exact location in time of the peaks must be found.
For this purpose, a polynomial fitting around TDB is performed. The fitting is applied on a stencil which dimension is computed as:

$$\text{Interpolation interval} = 2\,\frac{\text{Time(TDB)}-\text{Time(TDA)}}{\text{n}} \qquad (6)$$

where n=2 is a constant that was defined by means of tests on synthetic peaks. The peak position is defined as the maximum of the polynomial curve that best fits the raw signal, Fig. 10.

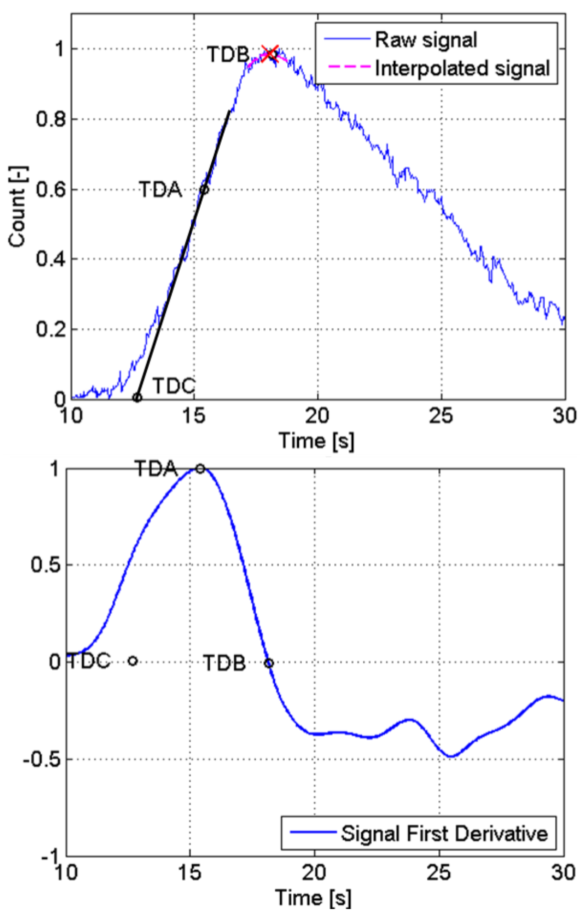

Figure 9: Polynomial fitting method

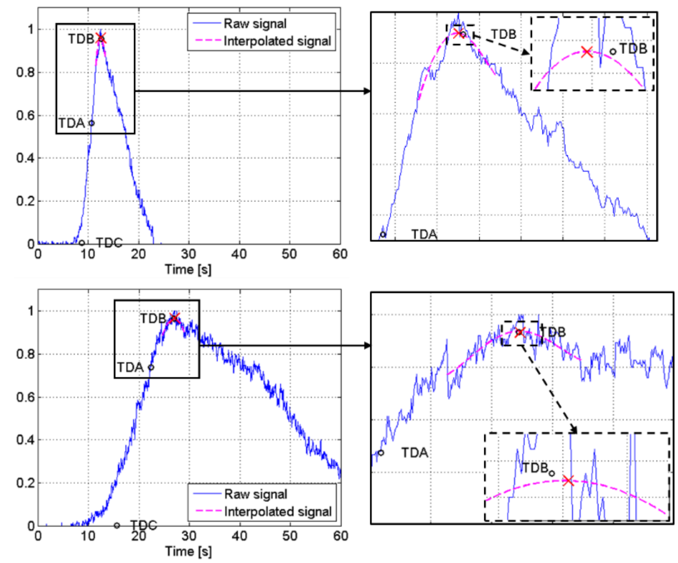

Figure 10: Examples of peak localization on two very different signals. Peak position is marked with the "X".

The polynomial coefficients are determined by a least squares procedure. The polynomial order can be user defined but a 4th order is normally the more robust solution. This evidence was obtained by several preliminary tests performed on samples of signal characterized by different shapes, intensity and noise content in order to assess the most reliable polynomial degree for the interpolation. As a result, the 4th order polynomial was the most consistent throughout the tests.
The activation time (i.e. the green peak location) of each pixel is saved on a multidimensional matrix of size X*Y*N*3, where X and Y are the image dimensions, N is the number of liquid crystals used in the mixture, and 3 is the total number of analyzed colors (namely red, green, and blue). Successively, each non-zero element of the matrix is validated by means of a hierarchical criteria algorithm. The validation procedure about the green peak position is based on the evaluation of the consistency about the time evolution of red and blue signals with respect to the green one. Indeed, the blue, green and red peaks must appear in a determined temporal sequence, depending upon the type of transient experiment (hot or cold temperature step).
The validated time matrices are finally de-warped and merged together in order to provide a final map of activation times on the whole geometry.
The T_b distribution map at each time interval is computed with the finite element method based on the Laplace diffusion equation [9].

$$\frac{\partial^2 T}{\partial x^2} + \frac{\partial^2 T}{\partial y^2} = 0 \qquad (7)$$

The T_b computation starts from the loading of the thermocouples readings obtained thanks to the Ni-cRIO. By doing so, the temperature evolution of the fluid during the test can be reconstructed at each thermocouple position. For this purpose it is necessary to locate the thermocouples in the image space. This operation is performed with a self-developed pick point tool that allows one to pick directly from the de-warped image the position of the thermocouples. Then, a mask is defined on the same image and is used to identify the edges of the computational domain. A commercial mesher toolbox and finite element solver (Matlab) are applied for the T_b computation on the domain. Neumann boundary conditions (adiabatic wall) are imposed on the mesh edges while Dirichlet boundary conditions are imposed on the mesh nodes that surround the thermocouples locations.

As a final step, the heat transfer coefficient on the passage surface is computed following the well-known Duhamel approach [10]:

$$T_w = T_0 + \sum_{i=1}^{n} \left(T_{b,i} - T_{b,i-1}\right) \times \left[1 - exp\left(\frac{h^2(t-\tau_i)}{\rho ck}\right) erfc\left(\sqrt{\frac{h^2(t-\tau_i)}{\rho ck}}\right)\right] \qquad (8)$$

where the data used for the integration are the data contained in the activation time matrices and in the T_b solution.

CONCLUSIONS

The design and operation of a new rig for heat transfer measurements in rotation have been presented. The challenging task to apply transient liquid crystal in rotation and on large models posed many technical issues that have been solved. The key features of the adopted solutions are described.

The implementation of the vision hardware, the acquisition and rig control systems are also described in detail.

New strategies have been adopted to process the acquired data (TLC images) with particular reference to the processing of highly distorted images and to the peaks finding procedure.

The rig and test procedure have been successfully commissioned with tests on a three pass model. The details can be found in another contribution to ASME Turbo Expo 2016 [11].

PERMISSION FOR USE

REFERENCES

[1] Wright, L.M., Liu, Y.H., Han, J.C. and Chopra, S., 2008, “Heat Transfer in Trailing Edge, Wedge-Sharped Cooling Channels Under High Rotation Numbers”, Journal of Heat Transfer, Vol. 130 / 071701-2

[2] Huh, M., Lei, J. and Han, J.C, 2010, “Influence of channel orientation on heat transfer in a two-pass smooth and ribbed rectangular channel (AR=2:1) under large rotation numbers”, ASME Turbo Expo 2010, GT2010-22190

[3] Astarita, T., Cardone, G., de Luca, L. and Carlomagno, G.M., 2015, “Some Experimental Investigations on Gas Turbine Cooling Performed with Infrared Thermography at Federico II”, International Journal of Rotating Machinery, Volume 2015/890414

[4] Mayo, I., Arts, T., El-Habib, A. and Parres, B., 2014, “Two-Dimensional Heat Transfer Distribution of a Rotating Ribbed Channel at Different Reynolds Numbers”, Journal of Turbomachinery, Volume 137 / 031002

[5] Waidmann, C., Poser, R., von Wolfersdorf, J., Fois, M. and Semmler, K., 2013, “Investigation of Heat Transfer and Pressure Loss in an Engine-Similar Two-Pass Internal Blade Cooling Configuration”, ETC 2013 / 109390

[6] Domaschke, N., von Wolfersdorf, J.and Semmler, K., 2009, “Heat transfer and pressure drop measurements in a rib roughened leading edge cooling channel”, Proceedings of ASME Turbo Expo 2009, GT2009-59399

[7] Kunstmann, S., von Wolfersdorf, J. and Ruedel, U., 2009, “Heat transfer and pressure loss in a rectangular one-side-ribbed channels with different aspect ratio”, Proceedings of ASME Turbo Expo 2009, GT2009-59333

[8] Ekkad, S. and Han, J.C., 2000, “A transient liquid crystal thermography technique for gas turbine heat transfer measurements”, Meas. Sci. Technol. 11 957-968

[9] Poser, R., von Wolfersdorf, J. and Lutum, E., 2007, “Advanced evaluation of transient heat transfer experiments using thermochromic liquid crystals”, Journal of Power and Energy, Vol 221 DOI: 10.1243/09576509JPE464

[10] Ireland, P.T. and Jones T.V., 2000, “Liquid crystal measurements of heat transfer and surface shear stress”, Meas. Sci. Technol. 11 969-986

[11] Pagnacco, F., Furlani, L., Armellini, A., Casarsa L. and Davis, A., 2015, “Rotating heat transfer measurement on a multi-pass internal cooling channel - II Experimental tests”, Submitted to ASME Turbo Expo 2016 GT2016-56307